ADVANCED FUNCTIONAL MATERIALS
www.afm-journal.de

Multi-Material 3D Microprinting of Magnetically Deformable Biocompatible Structures

Roxane Pétrot, Thibaut Devillers, Olivier Stéphan, Orphée Cugat, and Caterina Tomba**

Two-photon polymerization (2PP) allows precise 3D printing at the micrometer scale, and by associating it with magnetic materials, the creation of remotely actuatable micro-structures. Such structures attract a growing interest for biomedical applications, thanks to their size and to the biocompatibility of some photoresist materials. Gelatin methacryloyl (Gel-MA) is one such material, and can be used to create physiological scaffolds for cell culture. Here, the physico-chemical properties of two resins are exploited, the first being a silica-based hybrid polymer, the OrmoComp, and the second a Gel-MA-based hydrogel. A 2PP manufacturing protocol is defined and designed to print both materials in succession as a single structure, which is then linked to a neodymium-iron-boron (NdFeB) magnetic bead for actuation. By this combination, a magnetically deformable 3D culture substrate is created to study cells in an environment that mimics soft, curved, and dynamic properties of tissues in vivo. The structure is actuated via an external magnetic field and bends back and forth along its longest axis. Lastly, preliminary cell culture trials are conducted showing the proliferation of cells on the structures.

1. Introduction

Microprinting by two-photon polymerization (2PP) allows the manufacturing of microscale complex structures.[1] Numerous materials can be used, from polymer resins to protein-based photoresists, allowing fabrication in short amounts of time, from minutes to hours. 2PP micro-printing involves moving a laser's focal point through the photosensitive resin according to a file of pre-determined points, or voxels. The resin hardens at these voxels, building a 3D structure. To improve printing quality, the voxels' location and the laser power must be optimized. The uncured resin is then washed using an appropriate solvent.

2PP opens the possibility to create functional devices at the microscale,[2,3] either from the material properties themselves or by actuating the printed structures, for example via optical tweezers,[4,5] or magnetic particles and fields.[6–10] Such micro-actuators can be used for cell manipulation,[4,11,12] drug delivery,[6,13] or mixing in micro-fluidics[14,15] for example. Most of these micro-actuators are printed using polymer- or monomer-based resins, often chosen for their mechanical properties and ease of use for 2PP.

Biocompatible hydrogels, such as gelatin methacryloyl (Gel-MA)[16] or polyethylene glycol diacrylate (PEGda) ,[17,18] are also used for 2PP,[19–21] mostly to create scaffolds and other structures for cell culture. The mechanical properties of these hydrogels, thus their rigidity, can be adjusted by changing their massic concentration and the printing parameters. Gel-MA hydrogels have a Young's modulus ≈10–100s kPa,[16,22] while PEGda hydrogels are in the 1–10s MPa.[23,24]

R. Pétrot, T. Devillers
Institute of Engineering Univ. Grenoble Alpes
CNRS, Grenoble INP
Institut Néel
38000 Grenoble, France

R. Pétrot, O. Cugat
Institute of Engineering Univ. Grenoble Alpes
CNRS
Grenoble INP
G2Elab
38000 Grenoble, France

O. Stéphan
Univ. Grenoble Alpes
CNRS
LIPhy
38000 Grenoble, France
E-mail: olivier.stephan@univ-grenoble-alpes.fr

C. Tomba
Univ Lyon, CNRS, INSA Lyon, Ecole Centrale de Lyon
Université Claude Bernard Lyon 1
CPE Lyon
INL, UMR5270, 69622 Villeurbanne, France
E-mail: caterina.tomba@cnrs.fr

The ORCID identification number(s) for the author(s) of this article can be found under https://doi.org/10.1002/adfm.202304445

DOI: 10.1002/adfm.202304445

Moreover, extracellular matrix proteins such as collagen or fibronectin can be coupled to the base to improve the hydrogel's compatibility with cells by reproducing physico-chemical properties of in vivo environments.[25,26] This makes structures physiologically closer to real tissue than usual commercially available polymer resins. Printing multi-material structures allows to exploit the complementary properties of each material, but very little work has been done on the use of 2PP for such hybridization of materials.

In the literature, two main strategies have been considered, based on the same principle. One approach is to print with the first material, rinse the uncured resin as usual, then deposit the second material, print, and rinse again.[27–29] The other approach consists in using a microfluidic system to pump photosensitive resins and solvents successively around the sample. This second strategy allows printing multiple resins in multiple steps without moving the sample.[30]

Some teams have demonstrated the feasibility of printing by 2PP with several resins for manufacturing protein cell scaffolds with a polymer backbone[29] and complex multi-material structures.[27] However, this has never been used before to make deformable and actuable structures.

Cells are most often cultured on flat Petri dishes or hydrogel substrates, but some more complex environments have been created to get closer to in vivo conditions, for example, static 3D structures that mimic intestinal villi[25,26,31] or actively folded 2D substrates.[32,33] Here, we want to manufacture a 3D deformable structure for cell culture, to study the behavior of cells in curved environments and with dynamic and reversible movements.

Using a photoresist made of Gel-MA and collagen[34] creates an environment beneficial for cell growth[21] with physico-chemical properties close to real tissue. However, as gelatin-based hydrogels are very soft, they need some support to ensure overall stability and predictable deformation: for this, we use an internal skeleton made out of OrmoComp, a commercial silica-based photoresist. The challenge is then to successfully print both materials one after the other into one structure.

2. Building a Hybrid Structure for Cell Culture

The global hybrid structure is made of three parts, each made of a different material. First is an inner skeleton made of OrmoComp, a hybrid organic-inorganic photopolymer, glass-like when hardened; then an outer envelope made of a photosensitive composition made with Gel-MA, collagen, and a water-soluble ruthenium(II) photoinitiator; and finally a NdFeB magnetic bead for actuation, 30 to 50 µm in diameter and initially not magnetized (**Figure 1**). Combining the material properties of the two different photoresists (OrmoComp and gelatin-collagen hydrogel) produces a structure that is structurally solid and a suitable medium for cell growth. Here, we have designed and built a hybrid structure that can bend in the x/y plane thanks to the magnetic bead at its end. This direction of bending was chosen both to deform the structure in one plane (instead of out-of-plane), and for ease of viewing with an optical microscope.

The two printed parts of the structure, the skeleton, and the envelope are very different; we will first describe the skeleton, then the resin hybridization process, which involves printing the hydrogel envelope onto the OrmoComp skeleton. The fabrication

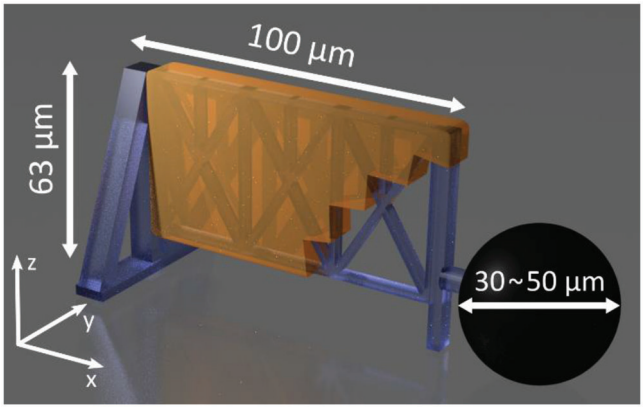

Figure 1. 3D rendering of the global structure. Blue: internal OrmoComp skeleton; orange: hydrogel envelope (cutout to reveal the skeleton); black: magnetic bead for actuation.

method of the link binding the magnetic bead to the structure was already described elsewhere.[35]

OrmoComp has Young's modulus ≈ 1 GPa,[36] rendering the skeleton rigid yet bendable with elastic deformations. It also has strong adhesion to both the glass coverslip it is printed on and the magnetic bead. The gelatin-collagen envelope provides a good surface for cell growth and is a soft material (E ≈ 100 kPa[16]) allowing the printed structure to bend freely in all directions. Lastly, the NdFeB bead is magnetized along X and provides the bending moment when subjected to an external magnetic field.

2.1. OrmoComp Skeleton

2.1.1. Design

The skeleton constitutes an armature for the hydrogel envelope and cells, and must therefore meet some specifications:

- be stable and robust enough to withstand the rinsing of the OrmoComp and the deposition of the heated liquid hydrogel droplet;
- flexible so as to allow the deformation of the complete structure;
- printing fast enough to build multiple skeletons in a few hours. The printing duration is directly correlated to the number of laser positions (voxels) where crosslinking occurs, which is determined by the overall size of the structure.

Based on these criteria, the skeleton is composed of two main parts: a main pillar, supported by two tilted beams so as to withstand deformation stresses during construction and washing; and from this pillar a long lattice body, allowing the skeleton to bend along the main axis, around Oz, while limiting twisting, and keeping printing time < 1 h per item.

The torque experienced by the permanent magnet bead when submitted to a magnetic field is transmitted to the beam through the printed link, and considered as a mechanical torque along Oz:

$$\vec{\tau} = \overrightarrow{m} \times \vec{B} = M.V\vec{x} \times B\vec{y} = M.V.B\vec{z}$$
$$\tau = 42.10^{-11} N.m \quad (1)$$

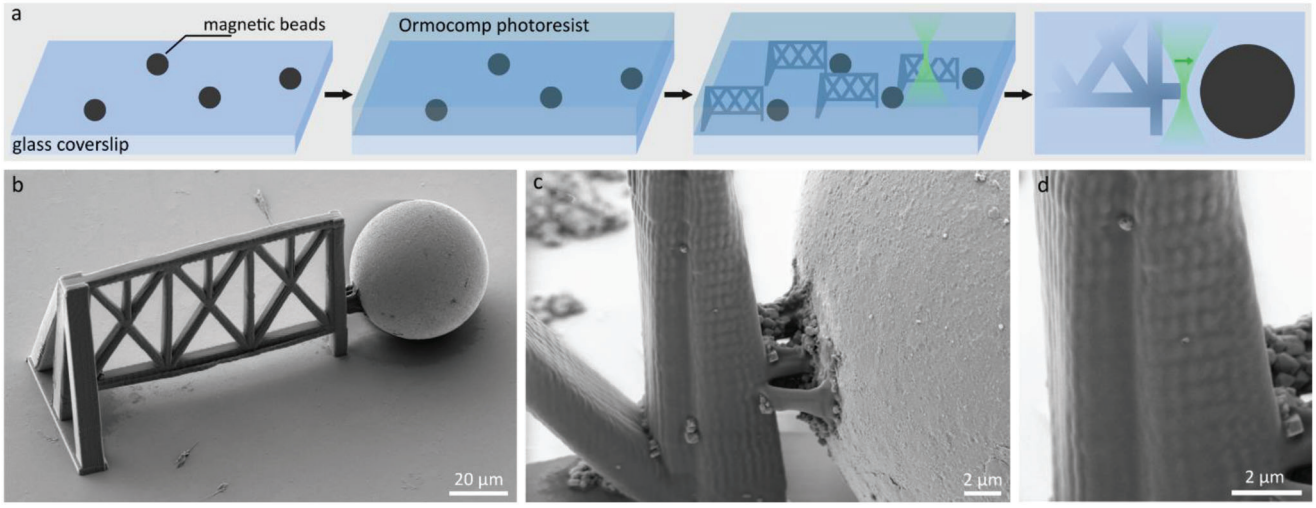

Figure 2. Printing of the OrmoComp skeleton bound to a NdFeB magnetic bead. a) Schematics showing the printing process: the beads are first dispersed on the coverslip and a drop of resin is deposited on top. The structures are then built next to magnetic beads, and linked to them. b) scanning electron microscope (SEM) image of a magnetic bead attached to the OrmoComp skeleton. c) Zoom on the OrmoComp-made link. d) Details of the voxels on the structure.

with m the bead's magnetic moment,
$B = 50$ mT the external magnetic flux density,
$\mu_0 M = 740$ mT the bead's magnetization,
and $V = 1.4.10^{-14} m^3$ its volume (radius 15 µm).

Using this value, we carried out simulations to determine the lattice's optimal thickness (along y) and the structure's deflection under the applied magnetic field. A lattice thickness of 4 µm is thick enough to guarantee a good printing quality (Figure S1, Supporting Information) while allowing full bending of the structure keeping Von–Mises stress under 100 MPa, which means the deformation is elastic.

2.1.2. Printing of the Skeleton

Based on the fabrication process shown in **Figure 2**a, the OrmoComp skeletons were printed with a laser power of ≈500 µW with a laser exposure time of 2 ms for each laser position (voxel).

The model is sliced with a voxel position every 0.12 µm in the x/y plane and 0.2 µm along z, and filled with horizontal lines every 1 µm along x and spaced by 0.5 µm in z (Figure 2b). These values ensure that the print is strong enough to remain upright when the hydrogel drop is added for the second step of manufacturing. The skeleton is printed next to a magnetic bead that is then attached using the technique previously developed[35] (Figure 2a), by printing multiple lines going from the structure to the bead. The link between the skeleton and the bead comprises multiple lines to improve adhesion (Figure 2c). The structures are then washed in acetone for 10 min and dried in an acetone-heavy environment. Figure 2d shows the structuration of the surface at the sub-micrometer scale, due to the printing parameters.

2.1.3. Actuation

Simulations on the skeleton alone show that the structure can be deformed to its maximum capacity, up to a semicircle, without affecting skeleton integrity (**Figure 3**a).

In the simulations, the main pillar is fixed and a torque along z is applied to the bead, using increasing values from 10 to 100×10^{-11} N.m. The beads are magnetized at saturation (μ_0M = 740 mT for isotropic NdFeB[37]) to ensure reproducibility and maximum deformation.

Here, the actuation field is generated and oriented by rotating an external permanent magnet (Figure 3b). The magnetic field around the structures is between 50 and 100 mT, depending on magnet orientation, distance, and manipulation.

When the external magnetic field rotates, the beads also rotate so as to align with the field, thus bending the structures along their length. The field may also be generated by electromagnets, which allows for greater control of the magnetic field but is more complex to implement.

Experimentations show that the deflection is in good agreement with simulations. A difference is only noticeable at maximal deformation: the link, being thinner, bends more than the structure yet remains elastic.

2.2. Building the Envelope Around the Skeleton

The gelatin-collagen envelope is then printed onto the OrmoComp skeleton. To this end, a drop of the gelatin-based resin heated to 40 °C is deposited on the sample. The hydrogel is solid at room temperature and liquefies ≈ 40 °C. However, the resin needs to be hardened and partially evaporated for printing. When printing too early, before the gelatin-based resin is hardened, a "cloud-like" defect appears around the structures, which contains some partially polymerized resin (Figure S2, Supporting Information). This defect enshrouds the structures, preventing their actuation, as well as blocking the cells from accessing and adhering onto the printed substrate. Upon solidification, the resin drop exerts stress on the OrmoComp skeletons, which then collapse, making it impossible to print the hydrogel envelopes around them.

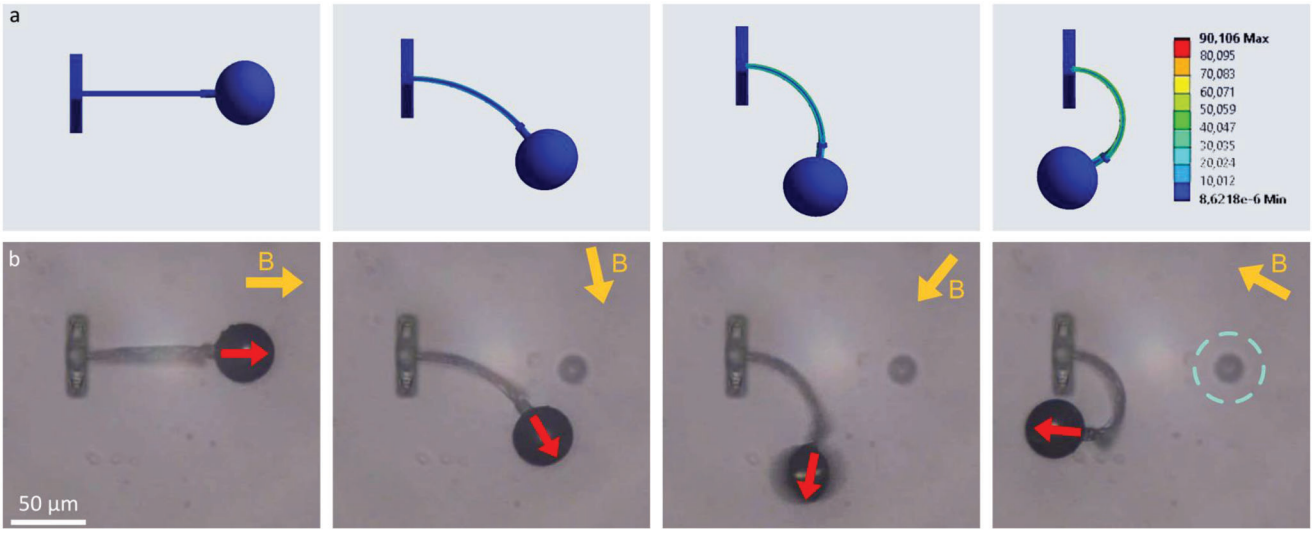

Figure 3. Magnetic actuation of the skeleton. a) Non-linear finite elements simulation of the beam deflection and associated Von–Mises stress (values expressed in MPa in the color scale). b) Optical microscope images of the skeleton deformation under a magnetic field (yellow arrow: external magnetic field; red arrow: bead magnetization; circled area: printing artifact, which may block the movement).

To solve this issue, we have optimized a printing protocol for hybrid structures (**Figure 4**a): First, the OrmoComp skeletons are printed and washed in the usual conditions (acetone). Gelatin-based resin is liquefied at 40 °C, and the sample is positioned on the hot plate to be at the same temperature; then a drop of liquid resin is deposited on the heated sample. The sample is kept at 40 °C for 30 min, allowing the drop to partially evaporate while staying almost liquid. Eventually, the evaporation stops, and the sample is cooled back to room temperature, letting the drop harden fully.

The envelope is then built using the micro-printing set-up, and washed in PBS (Phosphate-Buffered Saline) at 40°C for 30 min to remove uncured hydrogel materials. Finally, the beads are magnetized as previously described. Figure 4b,c shows finished multi-material structures, from two different angles. In Figure 4c, the envelope is not well centered on the skeleton, being

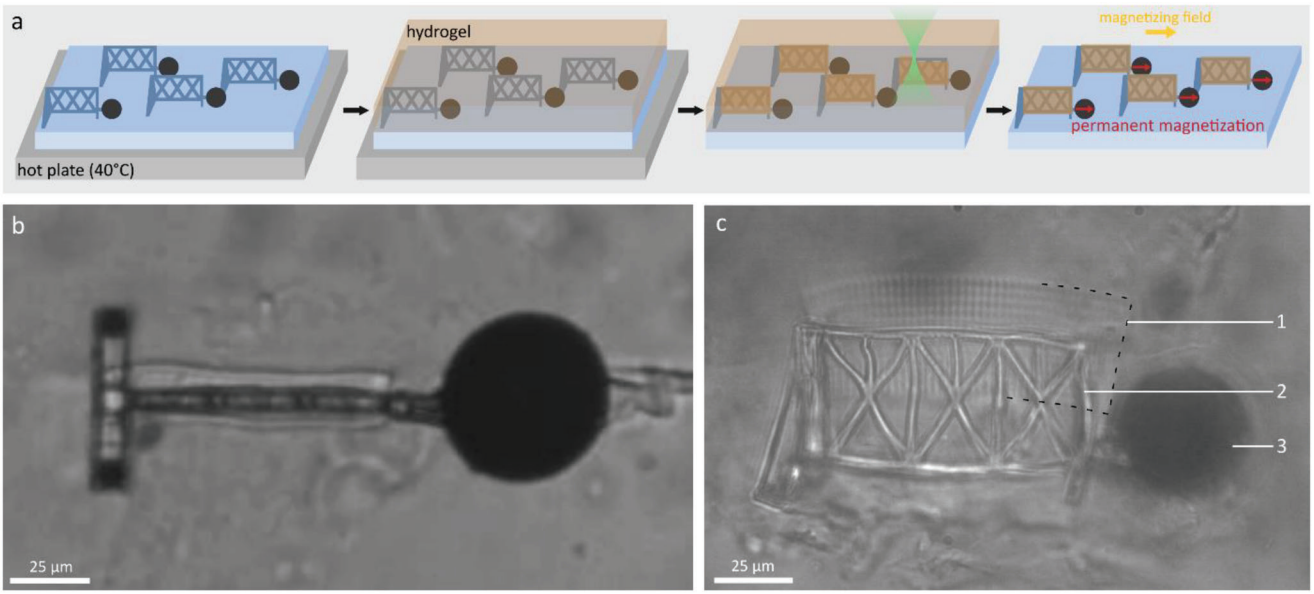

Figure 4. Printing the collagen envelope. a) Schematics showing the printing process: the sample is heated to 40 °C and a drop of liquid hydrogel is deposited on top of the structures. The system is kept at 40 °C for 30 min, then cooled back to room temperature. The envelopes are then printed around the skeletons, and washed in PBS. Lastly, the beads are magnetized. b) Optical microscope top–down view of a printed full structure (skeleton, envelope, magnetic bead). c) Side view of a purposefully knocked down structure. 1: hydrogel envelope, 2: OrmoComp skeleton, 3: NdFeB bead.

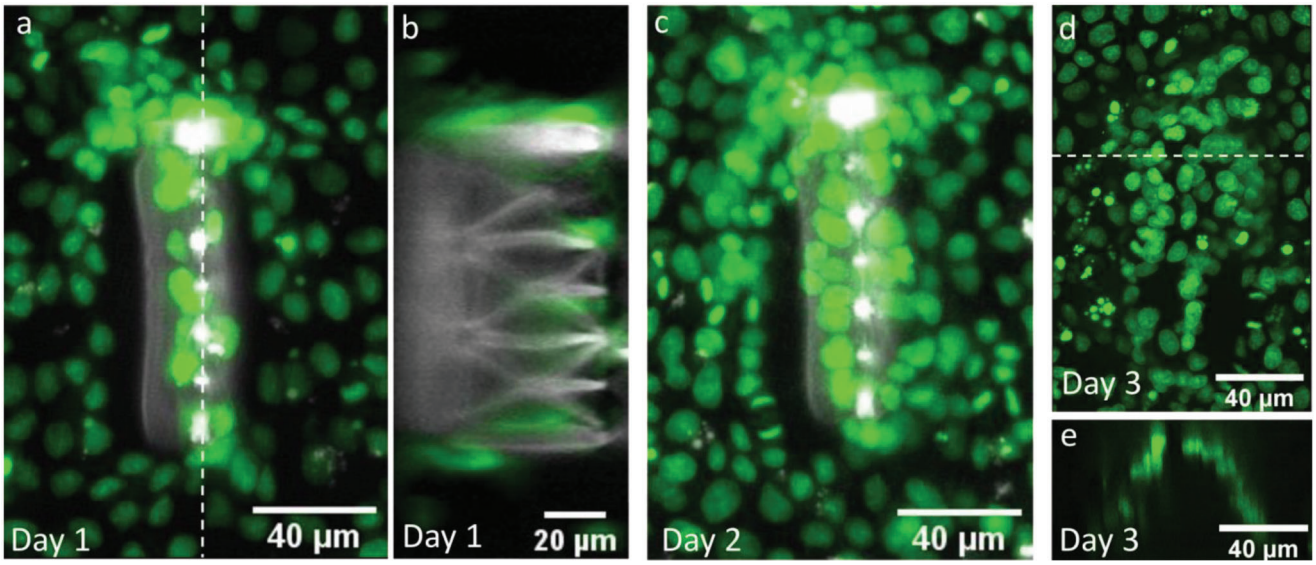

Figure 5. Cell culture on the hybrid structures, with MDCK cells. Green = cell nuclei, white = OrmoComp structure and gelatin-collagen-based hydrogel envelope. a,c,d) Maximum-intensity z-projections at Day 1 (a), Day 2 (c), and Day 3 (d) of culture. b) Confocal XZ cross-section on Day 1. The dashed lines in a and d indicate the position of the cross-section shown in (b,e), respectively. e) Confocal YZ cross-section view across the main axis of the structure (dashed line in d).

too high in z, and swelling is noticeable on the free part: this is an intrinsic feature of the hydrogel, which can swell ≈ 1.6 times its initial size.

3. Cell Culture

One main goal of the approach developed in our research is to use these deformable structures as substrates for cell culture. Indeed, their movement and curvature aim to replicate real soft tissue conditions, which deform with the body. Cultivating cells on such supple and controllable substrates allows to study them in an environment closer to in vivo physical constraints than classical culture in Petri dishes or in standard flat or structured, static substrates.

Collagen and gelatin are commonly used as substrates for cell culture: our formulation was already successfully used to build 3D gelatin-collagen matrices and to grow cells in them.[21]

The experiments presented here are still in the early stages of development. MDCK (Madin–Darby Canine Kidney II) cells were chosen for the preliminary adhesion assays on the hybrid structures as model cells of epithelium, which form well-organized cell monolayers. Indeed, MDCK cells were proven to be responsive to substrate curvature and stress [32,33] and are therefore well suited for mechanobiology studies. To validate the biocompatibility of the structures, including the adhesion and the growth of the cells, these were deposited onto the 3D printed structures without a magnetic bead and cultured at 37 °C and 5% of CO_2 for 3 days (**Figure 5**). The cells have proliferated, showing that the multi-material structures are a suitable substrate for cell culture. Figure 5d shows that the cells follow a curved profile, instead of the expected rectangle shape of the envelope: this is due to printing issues with the partially polymerized gelatin-collagen hydrogel around the printed envelope. Although the viability of gelatin-collagen substrates has been demonstrated up to day 15 after seeding ,[21] the long-term viability of the hybrid substrates including ormocomp and magnetic bead has not been assessed yet beyond day 3 and should be studied in the next work.

4. Conclusion

In order to create a culture environment that mimics in vivo conditions, we have developed and fabricated hybrid OrmoComp and collagen-gelatin structures, which can be magnetically deformable; we have studied their actuation, then validated the cell culture on these hybrid structures. The structures are composed of two parts successively printed with two different materials and a magnetic bead bound through 2PP.

To combine these two materials in 2PP, we developed a suitable manufacturing protocol that allows the collagen-gelatin drop to dry without applying much stress to the OrmoComp skeletons. The method consists in heating the sample while it dries, in order to prevent rapid gelation.

Magnetic actuation successfully deforms the structures completely and experimental results are in good agreement with the simulations. Work on in vitro cell culture is still in its infancy, but the results are encouraging. Actuation of the complete structure with cells should then allow to study the cells reaction to substrate deformation. Moreover, the fabrication of hybrid structures being mastered, we will also be able to work on the design and printing of other hydrogel structures, and at larger scales. These structures can be used either to replicate curved dynamic tissues in vivo such as the intestinal barrier or the lung bronchi and to conduct more investigations in the mechanobiology field, or for other applications in the micro-actuator field.

5. Experimental Section

Materials: The sol–gel photoresist used was an OrmoComp-based mixture, prepared by dissolving 6 mg of 1,3,5-tris(2-(9-ethylcabazyl-3)ethylene) benzene photoinitiator into 1 mL of dichloromethane, then mixing in 1 g of OrmoComp and letting the dichloromethane evaporate.

The collagen and gelatin-based hydrogel photoresist was prepared by mixing 10 mg of dichlorotris(1,10-phenantroline)ruthenium(II) hydrate with 1 mL of deionized water, then adding 200 mg of gelatin methacryloyl (gelatin from bovine skin, Sigma–Aldrich), and 30 mg of collagen (collagen from rat tail, Sigma–Aldrich). The mixture was then heated and stirred until fully homogeneous.

The magnetic beads were gas-atomized spherical NdFeB polycrystalline powders (MQP-S-11-9-20001, Magnequench). Wet sieving was used to separate them by size. The beads used were between 30 and 50 µm in diameter. Their magnetization was isotropic, saturating at 740 mT.

A macroscopic annular NdFeB permanent magnet was used for moving the magnetics beads and actuating the structures (external diameter 2 cm, height 1 cm, with a 4 mm axial bore). Its magnetization was 1.2 T (diametrally), generating fields of 10–120 mT at distances 30–5 mm.

Equipment: For fabrication of the structures, a Microlight two-photon polymerization 3D microprinter was used, combined with a Zeiss inverted microscope with a 100×/1.25 objective lens. The printer uses a pulsed Nd-doped yttrium aluminium garnet laser emitting at 532 nm, in the green.

Software: The objects were designed using FreeCAD and exported to stl files. The printer needs a file defining each voxel (laser position), so the stl files were then converted to printing files (slicing) using Sympoly v4 (by Microlight3D). The structures were then printed using Lithos (Microlight3D), the software that manages the printer.

Mechanical simulations were performed using Ansys Workbench 2022 R2, with the following values of density, Young's modulus and Poisson's ratio for the OrmoComp and the NdFeB respectively: 1.18 and 7.5, $1.3 \bullet 10^9$ and $200 \bullet 10^9$, 0.3 and 0.29.

The optical images were taken with µEye Cockpit. The 3D renderings were made with Blender 2.78c.

Beads Magnetization: The beads were magnetized using a lab-made unipolar magnetic pulse generator. This coil emits a pulsed field of 4 T, which magnetizes the beads fully. After printing the structures, the glass slide ≈ 1 mm was cut from them, so that the sample could be brought vertically as close as possible to the coil, with the skeletons oriented along the coil's central axis.

Actuation: The structures were magnetically actuated by rotating the aforementioned macroscopic magnet 5–10 mm from the structures; experiments were carried out under an optical microscope.

Cell Culture: Madin Darby canine kidney II H2B-GFP (MDCK) cells were cultured in DMEM supplemented with 10% fetal bovine serum (FBS, Gibco, ref. n° 10270106), 1% Penicillin–Streptomycin (PS, Gibco, ref n° 15140122) and 1% non-essential amino acids (NEAA, Gibco, ref. n° 11140035), at 37 °C and 5% CO_2. After trypsinization, cells were seeded onto the 3D printed substrates and let for adhesion in the incubator for 24 h before imaging. At 3 days of culture, cells were chemically fixed with 4% formaldehyde (PFA, Sigma–Aldrich, ref. n°F8775) in PBS for 20 min, washed three times with PBS, and kept in PBS at 4 °C until imaging. MDCK H2B-GFP was kindly provided by H. Delanoë-Ayari (ILM, France).

Imaging (SEM, Fluorescence): A ZEISS Ultra+ scanning election microscope was used for the SEM images, and the structures were coated with a 15 nm thick gold layer.

Live cells were observed with an upright DM6 microscope Leica Thunder Imager 3D Cell culture with a water immersion 25x objective NA 0.95 (HC Fluotard L Visir dipping, Leica). Confocal images of fixed cells were obtained using an inverted Yokogawa/Nikon Spinning disk confocal microscope with a 40x objective NA 0.95 (Plan Apo Lambda 40X, Nikon).

Supporting Information

Supporting Information is available from the Wiley Online Library or from the author.

Acknowledgements

The authors thank L. Gredy for assistance with gelatin-collagen printing and Microlight3D for discussions and free assistance with the 3D microprinter. They also thank the NanoLyon (INL, France) and the ILM Tech facilities for the access to the microscopes and S. Monnier and E. Bastien (ILM, France) for their technical support. The authors also thank the Pumag project for providing the pulsed magnetic field generator. This work was funded by the French state funds ANR-10-LABX-51-01 (Labex LANEF, Programme d'Investissements d'Avenir).

Conflict of Interest

The authors declare no conflict of interest.

Data Availability Statement

The data that support the findings of this study are available from the corresponding author upon reasonable request.

Keywords

3D micro-printing, cell manipulation, hybrid structures, hydrogels, magnetic actuation, micro-actuators, two-photon polymerization

Received: April 22, 2023
Revised: July 9, 2023
Published online: August 1, 2023

[1] S. Kawata, H.-B. Sun, T. Tanaka, K. Takada, *Nature* **2001**, *412*, 697.
[2] F. Rajabasadi, L. Schwarz, M. Medina-Sánchez, O. G. Schmidt, *Prog. Mater. Sci.* **2021**, *120*, 100808.
[3] J. Li, M. Pumera, *Chem. Soc. Rev.* **2021**, *50*, 2794.
[4] E. Gerena, S. Regnier, S. Haliyo, *IEEE Robot. Autom. Lett.* **2019**, *4*, 647.
[5] E. Avci, M. Grammatikopoulou, G.-Z. Yang, *Adv. Opt. Mater.* **2017**, *5*, 1700031.
[6] S. Tottori, L. Zhang, F. Qiu, K. K. Krawczyk, A. Franco-Obregón, B. J. Nelson, *Adv. Mater.* **2012**, *24*, 811.
[7] J. Giltinan, M. Sitti, *IEEE Robot. Autom. Lett.* **2019**, *4*, 508.
[8] X.-Z. Chen, M. Hoop, F. Mushtaq, E. Siringil, C. Hu, B. J. Nelson, S. Pané, *Appl. Mater. Today* **2017**, *9*, 37.
[9] J. Zhang, O. Onaizah, K. Middleton, L. You, E. Diller, *IEEE Robot. Autom. Lett.* **2017**, *2*, 835.
[10] H. Zhou, C. C. Mayorga-Martinez, S. Pané, L. Zhang, M. Pumera, *Chem. Rev.* **2021**, *121*, 4999.
[11] M. S. Sakar, E. B. Steager, D. H. Kim, M. J. Kim, G. J. Pappas, V. Kumar, *Appl. Phys. Lett.* **2010**, *96*, 043705.
[12] S. Kim, F. Qiu, S. Kim, A. Ghanbari, C. Moon, L. Zhang, B. J. Nelson, H. Choi, *Adv. Mater.* **2013**, *25*, 5863.
[13] L. Schwarz, M. Medina-Sánchez, O. G. Schmidt, presented at 2019 Int. Conf. on Manipulation, Automation and Robotics at Small Scales (MARSS), IEEE, Helsinki, Finland **2019**.
[14] U. G. Būtaitė, G. M. Gibson, Y.-L. D. Ho, M. Taverne, J. M. Taylor, D. B. Phillips, *Nat. Commun.* **2019**, *10*, 1215.
[15] H. Xia, J. Wang, Y. Tian, Q.-D. Chen, X.-B. Du, Y.-L. Zhang, Y. He, H.-B. Sun, *Adv. Mater.* **2010**, *22*, 3204.
[16] K. Yue, G. Trujillo-de Santiago, M. M. Alvarez, A. Tamayol, N. Annabi, A. Khademhosseini, *Biomaterials* **2015**, *73*, 254.
[17] T. Wloka, S. Czich, M. Kleinsteuber, E. Moek, C. Weber, M. Gottschaldt, K. Liefeith, U. S. Schubert, *Eur. Polym. J.* **2020**, *122*, 109295.

[18] E. Käpylä, T. Sedlačík, D. B. Aydogan, J. Viitanen, F. Rypáček, M. Kellomäki, *Mater. Sci. Eng., C* **2014**, *43*, 280.
[19] X. Wang, X.-H. Qin, C. Hu, A. Terzopoulou, X.-Z. Chen, T.-Y. Huang, K. Maniura-Weber, S. Pané, B. J. Nelson, *Adv. Funct. Mater.* **2018**, *28*, 1804107.
[20] A. Ovsianikov, A. Deiwick, S. Van Vlierberghe, M. Pflaum, M. Wilhelmi, P. Dubruel, B. Chichkov, *Materials* **2011**, *4*, 288.
[21] B. van der Sanden, L. Gredy, D. Wion, O. Stephan, *Acta Biomater.* **2021**, *130*, 172.
[22] M. Sun, X. Sun, Z. Wang, S. Guo, G. Yu, H. Yang, *Polymers* **2018**, *10*, 1290.
[23] S. Gäbler, J. Stampfl, T. Koch, S. Seidler, G. Schüller, H. Redl, *Int. J. Mater. Eng. Innovation* **2009**, *1*, 3.
[24] Haryanto,S. Kim, J. H. Kim, J. O. Kim, S. Ku, H. Cho, D. H. Han, P. Huh, *Macromol. Res.* **2014**, *22*, 131.
[25] J. Creff, R. Courson, T. Mangeat, J. Foncy, S. Souleille, C. Thibault, A. Besson, L. Malaquin, *Biomaterials* **2019**, *221*, 119404.
[26] Y. Wang, D. B. Gunasekara, M. I. Reed, M. DiSalvo, S. J. Bultman, C. E. Sims, S. T. Magness, N. L. Allbritton, *Biomaterials* **2017**, *128*, 44.
[27] Q. Hu, G. A. Rance, G. F. Trindade, D. Pervan, L. Jiang, A. Foerster, L. Turyanska, C. Tuck, D. J. Irvine, R. Hague, R. D. Wildman, *Addit. Manuf.* **2022**, *51*, 102575.
[28] S. Engelhardt, *J. Laser Micro/Nanoeng.* **2011**, *6*, 54.
[29] S. Engelhardt, E. Hoch, K. Borchers, W. Meyer, H. Krüger, G. E. M. Tovar, A. Gillner, *Biofabrication* **2011**, *3*, 025003.
[30] F. Mayer, S. Richter, J. Westhauser, E. Blasco, C. Barner-Kowollik, M. Wegener, *Sci. Adv.* **2019**, *5*, aau9160.
[31] N. Torras, M. García-Díaz, V. Fernández-Majada, E. Martínez, *Front. Bioengin. Biotechnol.* **2018**, *6*, 00197.
[32] C. Tomba, V. Luchnikov, L. Barberi, C. Blanch-Mercader, A. Roux, *Dev. Cell* **2022**, *57*, 1257.
[33] S. Blonski, J. Aureille, S. Badawi, D. Zaremba, L. Pernet, A. Grichine, S. Fraboulet, P. M. Korczyk, P. Recho, C. Guilluy, M. E. Dolega, *Dev. Cell* **2021**, *56*, 3222.
[34] O. Stephan, L. Gredy, FR3049606B1, **2018**.
[35] V. Vieille, R. Pétrot, O. Stéphan, G. Delattre, F. Marchi, M. Verdier, O. Cugat, T. Devillers, *Adv. Mater. Technol.* **2020**, *22*, 2000535.
[36] C. Schizas, D. Karalekas, *J. Mech. Behav. Biomed. Mater.* **2011**, *4*, 99.
[37] "MQP-S-11-9-20001," can be found under https://mqitechnology.com/product/mqp-s-11-9-20001/.